Clustering of Satellite Sounding Radiances to Investigate Intense Low-Level Humidity Gradients

HENRY E. FUELBERG AND P. ANIL RAO

Department of Meteorology, The Florida State University, Tallahassee, Florida

DONALD W. HILLGER

NOAA/NESDIS Regional and Mesoscale Meteorology Branch, Cooperative Institute for Research in the Atmosphere, Colorado State University, Fort Collins, Colorado

(Manuscript received 20 June 1994, in final form 4 January 1995)

ABSTRACT

Satellite-derived profiles of temperature and dewpoint (retrievals) are obtained using radiance data from the Visible–Infrared Spin Scan Radiometer Atmospheric Sounder. Individual fields of view that are input to the retrieval algorithm must be horizontally averaged to provide suitable signal-to-noise ratios. This paper investigates three methods for performing this averaging: 1) a blocking approach that is employed operationally, 2) a manual procedure that seeks to maximize atmospheric gradients, and 3) an objective procedure called clustering that takes advantage of similarities in satellite measurements to avoid smearing the gradient information. The three techniques are examined on 10–11 July 1989 when intense gradients of humidity were present over the Florida peninsula.

Results show that the clustering scheme produced retrievals that were very similar to those obtained manually. Both schemes indicated strong humidity gradients in the lower troposphere. The blocking procedure produced less intense gradients. The retrieval information is used to examine conditions leading to fair weather on 10 July but intense thunderstorm development on 11 July.

1. Introduction

Satellite measurements are a source of information about mesoscale meteorological phenomena. The VISSR (Visible–Infrared Spin Scan Radiometer) Atmospheric Sounder (VAS) onboard the Geostationary Operational Environmental Satellites (GOES) provides radiance data in fields of view (FOVs) that are either approximately 7 or 14 km square depending on whether small or large detectors are utilized. These data have been used to generate vertical profiles of temperature and dewpoint (retrievals) at high horizontal resolution (e.g., Hayden 1988; Lee et al. 1983). Individual FOVs have signal-to-noise ratios that are unacceptably small for sounding purposes. To increase the ratios, multiple FOVs often are spatially averaged. However, this averaging can "smear" horizontal gradients in the resulting retrievals, particularly when the averaging is performed arbitrarily. Alternatively, Hillger and Purdom (1990) developed a "clustering" approach whereby FOVs are sorted by similarity in measurements. This methodology reduces the smearing of horizontal gradients, with spatial patterns of the retrieved data revealing more clearly the mesoscale airmass characteristics (Hillger and Weaver 1994).

This paper compares cluster-derived VAS retrievals produced at high spatial resolution with retrievals whose locations were obtained either manually or by the current operational objective technique. We then use the cluster retrievals to examine the preconvective environment over central Florida on 10–11 July 1989 when intense mesoscale humidity gradients were present in the lower troposphere.

2. Methodologies

We made VAS retrievals using the simultaneous physical algorithm that is employed operationally by the National Environmental Satellite Data and Information Service (NESDIS) (Hayden 1988). The VAS dwell sounding FOV data that were input to the algorithm were horizontally averaged using three different procedures. Our major objective was to compare the retrievals resulting from each of these approaches.

The first procedure was to manually select retrieval sites using a "man in the loop." That is, retrievals were made at selected sites after examining visible and infrared GOES imagery using the Man-computer Interactive Data Access System (McIDAS, Suomi et al. 1983). The retrieved temperatures and dewpoints were

Corresponding author address: Dr. Henry E. Fuelberg, Department of Meteorology, The Florida State University, Tallahassee, FL 32306-3034.

manually analyzed and edited, with additional retrievals made as needed. It was a time-consuming subjective process whose goal was to maximize horizontal gradients and avoid cloudy regions. We utilized 4 × 4 FOV nonoverlapping areas for averaging the radiance data around each retrieval site. This choice was appropriate since small detector (7 km) VAS channels consist of "Venetian blinds," that is, east-to-west data swaths of 32-km north–south width separated from each other by data voids of equal width. Thus, the 4 × 4 areas encompassed each north–south data strip without extending into the voids. An FOV was considered cloud contaminated if its 11-μm (window channel) brightness temperature was less than 288 K. These contaminated FOVs were deleted from the array of 16 possible points, with a minimum of eight remaining FOVs required to make a retrieval. Additional details about the manual procedure can be found in Hoepner and Fuelberg (1992).

The second procedure, called "blocking," is employed operationally by NESDIS (Hayden 1988). Retrieval sites and resulting averaging areas are arranged in a matrix, that is, without regard to meteorological features or data characteristics. We followed the NESDIS methodology by averaging radiance values from 11 × 11 small detector (7 km) FOVs to achieve a horizontal resolution of approximately 75 km. Cloud contaminated FOVs were detected using the same infrared threshold described above. A portion of each block always fell within the Venetian blinds, while some FOVs might be cloud contaminated. However, a minimum of 30 FOVs was required to calculate these retrievals.

The third procedure, clustering, categorizes the radiance data into groups having similar characteristics in all channels. Since the procedure is described thoroughly in Hillger and Purdom (1990), only highlights are presented here. Clustering maintains horizontal airmass gradients while minimizing the number of retrievals and maximizing the differences between them. Since the FOVs composing an individual cluster are similar to within the noise levels of the satellite sounding channels, one retrieval is sufficient to represent the entire cluster. Also, since differences between clusters are greater than the noise levels of the measurements, the retrieval for each cluster is significantly different from that for all other clusters.

The sizes of the clusters used for a given retrieval set are determined by the noise levels of the various sounding channels. These noise levels are estimated by spatial structure function analysis on the same satellite data employed for the clustering. A complete description of the structure function technique can be found in Hillger and Vonder Haar (1988).

VAS contains 12 infrared sounding channels. However, the number of independent variables being analyzed during the clustering process is significantly less than 12 because the VAS channels are highly redundant. This reduction is accomplished using principal component (PC) analysis, also called empirical orthogonal function (EOF) analysis, which creates independent functions representing the data in a more concentrated form (for enhanced simplicity or parsimony; Gauch 1993). We used the first three PCs that described over 90% of the variance in the VAS channels. To use PCs instead of satellite sounding channels directly, the noise levels of the PCs also had to be known. These noise levels were determined from the noise levels of the VAS channels using the same eigenvector transformation used to convert the satellite-sounding radiances to PCs.

The infrared threshold described above again was used to detect and avoid cloudy FOVs. A slight smoothing was applied to the PCs before clustering to add a small amount of spatial continuity to the data. Swain et al. (1981) have shown that classification accuracy can be improved by including contextual information. However, the inclusion of such contextual information in its most pure form is not a simple task. Our method to add some degree of contextual information was to employ a slight spatial smoothing of the PCs. This smoothing allowed us to take better advantage of spatial autocorrelations which, in turn, yielded improved spatial clustering of the satellite data. The end result of the clustering process was a set of 12 spatially averaged satellite brightness temperatures for each cluster. Our clusters contained between 16 and 193 FOVs.

Retrievals were produced for each averaging procedure using the FOV data as input to the simultaneous physical algorithm. First-guess profiles needed for the algorithm were obtained from morning radiosonde observations (raobs) at six sites over Florida and southeastern Georgia. Separate guess data were used for 10 and 11 July 1989. The raob at each site was interpolated to the 40 levels needed by the algorithm. Horizontal analyses were prepared manually for each level, with a guess profile for each VAS retrieval site obtained by subjective interpolation. Bias values traditionally are added to observed VAS brightness temperatures to reduce mean errors in the resulting retrievals (Hayden 1988). Our bias vectors were derived for the 2-day period of interest based on raobs from the Florida area.

3. Results

a. 10 July 1989

Synoptic analyses on the morning of 10 July 1989 indicate typical summertime conditions over Florida. Radiosonde-derived dewpoint temperatures at 850 hPa (Fig. 1a) vary only 7°C across the state. Central Florida is relatively dry, and precipitable water in the 900–800-hPa layer (Fig. 1c) ranges from 6.1 mm at Cape Canaveral to 10.7 mm at Key West. The ridge line of the Bermuda high extends across north Florida (Fig. 1a), with easterly winds covering much of the penin-

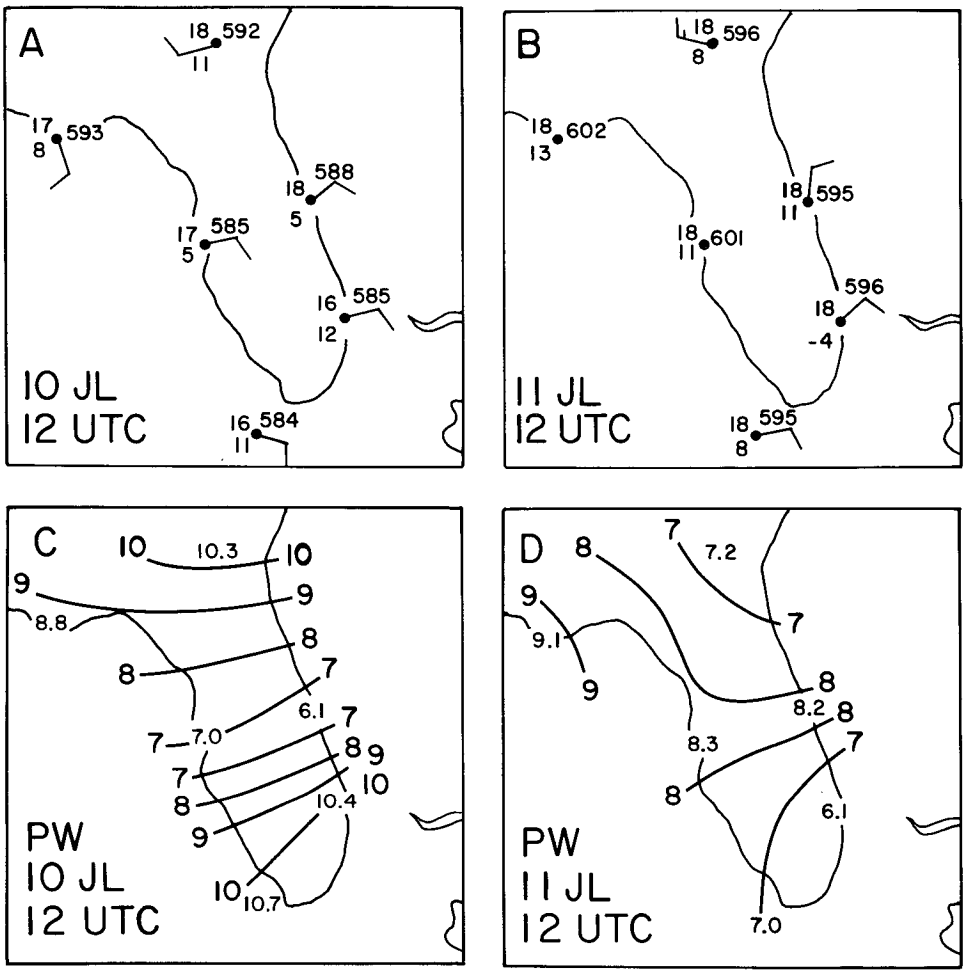

FIG. 1. Synoptic conditions at 850 hPa for 1200 UTC 10 July and 1200 UTC 11 July 1989. Temperatures and dewpoint temperatures in (a) and (b) are in degrees Celsius while heights are in meters (585 represents 1585 m). Full (half) barbs represent winds of 5 (2.5) m s^{-1}, respectively. Winds at Tampa and Apalachicola are missing on 11 July. Panels (c) and (d) contain precipitable water (mm) for the 800–900-hPa layer.

sula. Most dewpoints at the surface (not shown) are approximately 25°C, but values near 20°C stretch from near Cape Canaveral westward to Tampa. This relatively drier air over central Florida would be expected to suppress afternoon thunderstorm activity. No mesoscale humidity features can be detected by the relatively coarse radiosonde network (Figs. 1a,c). However, the VAS retrievals described in the following paragraphs do indicate pronounced mesoscale humidity gradients in the lower troposphere. Neither the radiosonde soundings nor the VAS retrievals reveal significant thermal features within the area (e.g., Fig. 1a). Therefore, these are not discussed further.

Figure 2a contains a subjective analysis of VAS-derived 850-hPa dewpoint temperatures for 1018 UTC 10 July. The manual (MAN) approach was used to select the 60 retrieval sites that are plotted. The most prominent feature is the very dry region located southwest of Cape Canaveral. The coldest (driest) value of −16°C is associated with intense horizontal gradients. This dry area was only partially detected by the synoptic-scale first-guess raob data (Figs. 1a,c); it results almost entirely from the VAS radiances. A region of humid air, with dewpoints reaching 15°C, is located along an east–west axis over northern Florida. There is a secondary dry area over extreme southern Georgia.

The dashed line in Fig. 3a represents the manually derived VAS retrieval for the driest point in Fig. 2a. Except for the lowest part of the sounding, the dry layer extends through most of the troposphere. The total column precipitable water (PW) for this retrieval is 10.5 mm. This is much drier than at location *M* (Fig. 3b), located approximately 160 km farther west, where the PW is 29.9 mm.

Several papers have evaluated VAS retrievals against radiosonde or dropwindsonde soundings (e.g., Velden et al. 1984; Jedlovec 1985; Hayden 1988; Franklin et al. 1990; Fuelberg and Olson 1991). The retrievals have

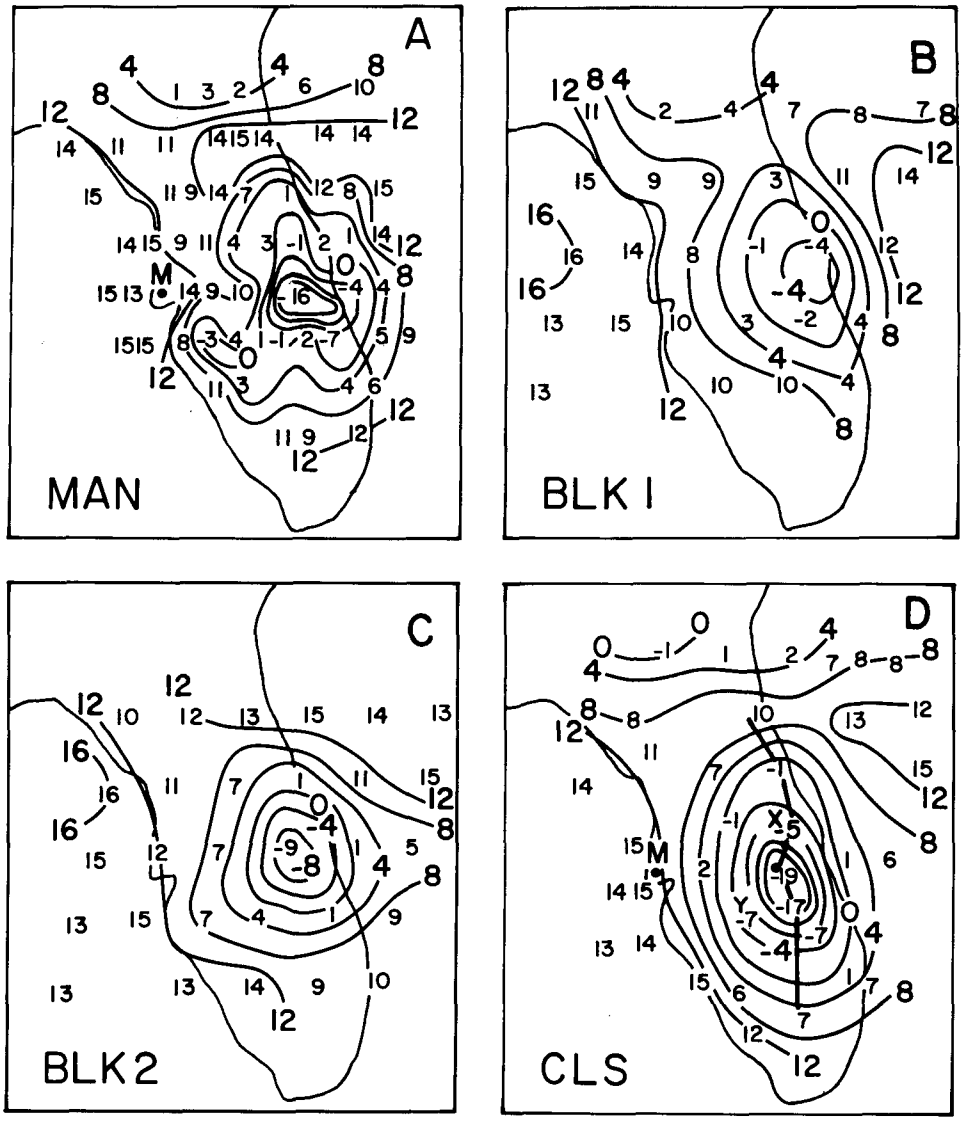

FIG. 2. Subjective analyses of VAS-derived dewpoint temperatures (°C) at 850 hPa for 1018 UTC 10 July 1989. Retrieval locations were selected (a) manually, (b) and (c) using two versions of blocking, and (d) using clustering. Point *M* in (a) and (d) and points *X* and *Y* in (d) are locations of soundings shown in Figs. 3 and 7. The solid line segments in (d) denote the axis of a cross section in Fig. 8a.

been found to suffer from poor vertical resolution, bias errors, and a dependence on the first-guess data. Conversely, the retrievals sometimes improved upon horizontal patterns and gradients of the first guess. Mesoscale radiosonde data were not available during this case. Therefore, we could not perform a similar evaluation of our retrievals. However, the current 850-hPa VAS dewpoint analysis (Fig. 2a) is consistent with the 800–900-hPa precipitable water analysis from the standard upper-air network (Fig. 1c). The retrievals denote intense mesoscale gradients that cannot be detected with the coarser network. In addition, mesoscale aspects of the VAS dewpoint analysis are similar to those of total column precipitable water (Fig. 4a). These values were obtained by Baker et al. (1993) using a split-window algorithm (Chesters et al. 1983, 1987) with multispectral imaging (MSI) data as input.

The block procedure was employed in two ways. In the first approach, we selected the 11 × 11 FOV averaging areas beginning in the upper-left corner of the data domain and continuing through the remainder of the region. This procedure, denoted BLK1, is depicted in Fig. 5a. A portion of each block would lie within a Venetian blind. We did not know in advance how the blocks would be located with respect to the dry region near Cape Canaveral seen in the MAN approach (Fig. 2a). However, this turned out to be a worst-case situation in which the dry area was divided between four

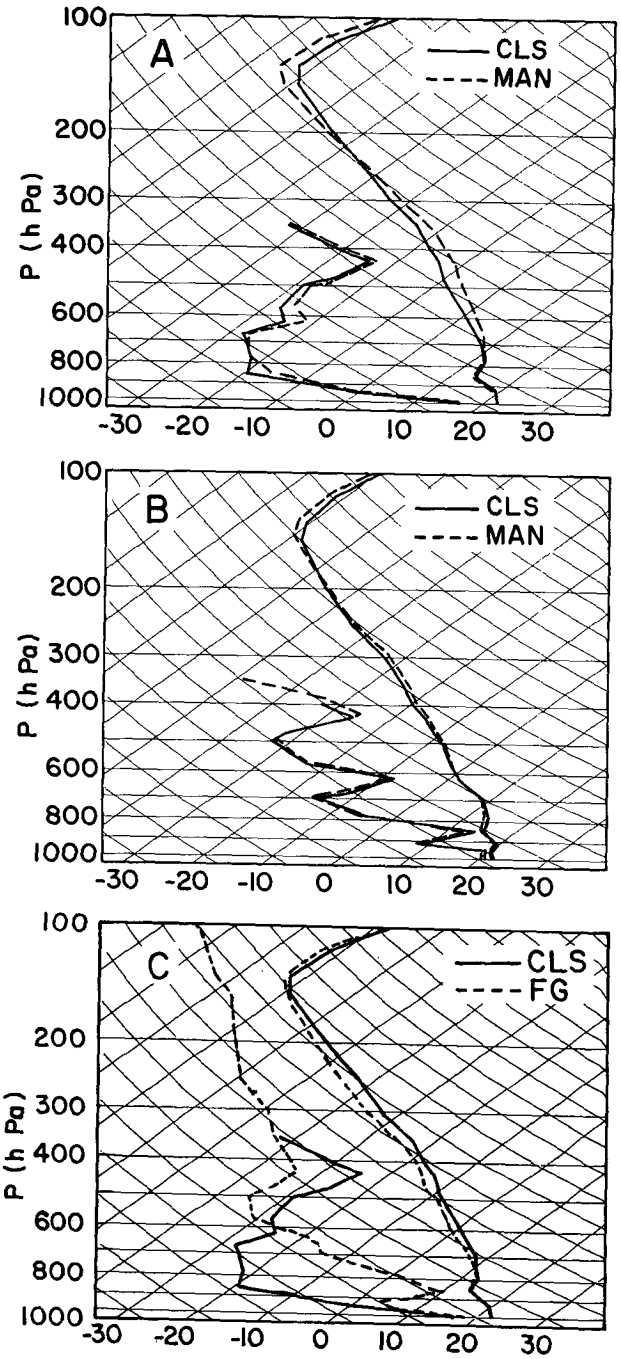

FIG. 3. Skew T–log$p$ diagrams of VAS retrievals. (a) The driest sites in Figs. 2a,d. (b) Point M in these same figures. (c) The driest clustered retrieval along with the first guess from which it was derived.

different blocks. The resulting 850-hPa dewpoint analysis is shown in Fig. 2b. The second approach (BLK2 in Fig. 5b) used information already gained from the manual procedure to center an 11 × 11 block over the dry area. The remaining block locations followed from this initial selection. The BLK1 and BLK2 configurations differ only in the locations of the averaging regions. They represent the worst and best blocking situations, respectively, that could occur on 10 July 1989.

Both block procedures reveal the dry area over east central Florida (Figs. 2b,c); however, its strength is reduced considerably from that of the MAN scheme. Specifically, the worst-case situation (BLK1) reduces its intensity to −4°C, instead of the −16°C from the manual approach. This difference is due mostly to the poor placement of the averaging areas, but also to using 11 × 11 matrices (as done by NESDIS) instead of the 4 × 4 regions employed in our MAN retrievals. With the help of hindsight (the BLK2 approach), the minimum dewpoint becomes −9°C. Both block procedures resolve to varying degrees the relatively moist area over North Florida. BLK1 also indicates the dry air over southern Georgia. These results show that the placement of block areas can produce considerable differences among

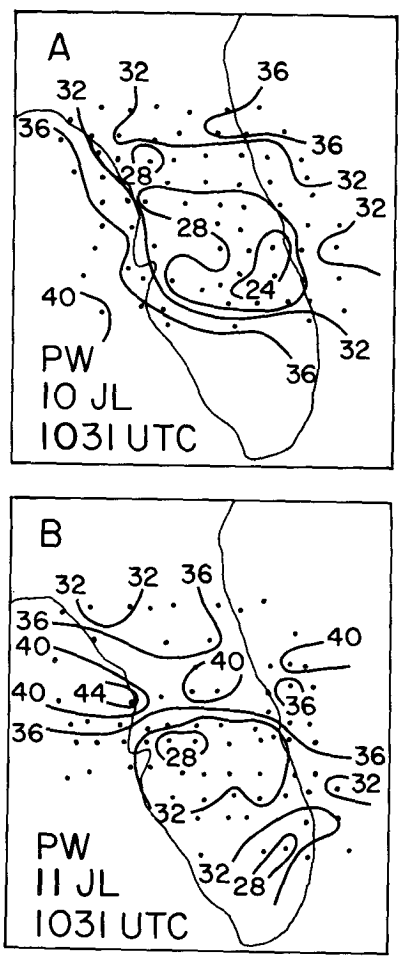

FIG. 4. Precipitable water (mm) for (a) 1031 UTC 10 July and (b) 1031 UTC 11 July 1989 obtained from a split-window channel algorithm (Chesters et al. 1983, 1987). Dots represent retrieval locations. The figure is adapted from Baker et al. (1993).

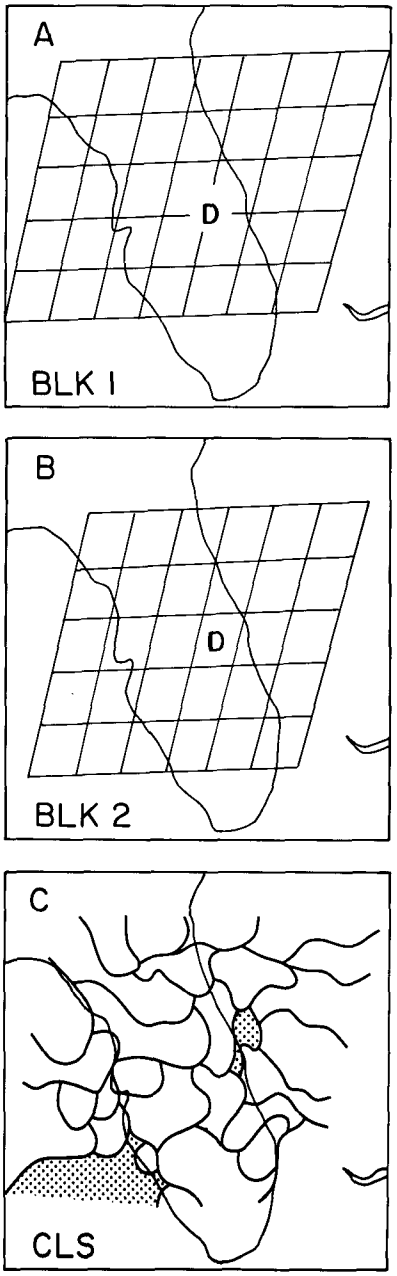

FIG. 5. Locations of the block averaging regions [(a) and (b)], where *D* represents the position of the driest manual retrieval in Fig. 2a. Areas comprising the cluster retrievals are in (c). Stippled areas denote clouds. A portion of each cluster and block was in a data void due to Venetian blinding that is not shown. Cluster and block boundaries have been interpolated across these gaps.

the resulting retrievals. In contrast to selecting the blocks manually, NESDIS functions in an operational environment, selecting the locations of the array of blocks without regard to meteorological features. The size (11 × 11) and shape of the blocks are fixed, except when cloud contaminated FOVs are deleted.

The analysis of cluster-derived (CLS) dewpoints at 850 hPa is given in Fig. 2d. Horizontal placements of the cluster areas are shown in Fig. 5c. There were 26 original clusters at this time; however, one cluster was not used since it consisted of several noncontiguous small regions. Conversely, 10 clusters either were large or consisted of two separate, major regions. To aid in analyzing the dewpoint fields, we prepared two retrievals for these cases—that is, one on either end of a large cluster area, or in each of the two separate areas. Although the cluster-derived brightness temperatures were identical in these cases, the first guess obtained for each specific location was used. This procedure has little influence on the resulting retrievals since the first guess data exhibit relatively weak gradients (Fig. 1).

The analysis of cluster-derived dewpoints (Fig. 2d) is similar to that obtained manually (Fig. 2a). Specifically, the CLS version contains a dry region southwest of Cape Canaveral, with the driest value being −19°C. This compares to −16° and −9°C for the MAN and BLK2 approaches, respectively. Both the MAN and CLS analyses indicate the moist zone stretching across northern Florida along with relatively drier air over extreme southern Georgia. Although the number of CLS retrievals is approximately half that of the MAN approach, the cluster versions differ from one another to within the noise contained in the VAS radiances. Thus, some of the manually derived retrievals may be redundant and may describe small-scale dewpoint features that cannot be justified by the noise characteristics of the radiance data. Retrievals based on clusters using only two PCs (not shown) instead of the three PCs presented here did not yield such close agreement with the manually derived retrievals. The three PCs explained 91% of the variance in the VAS channels, whereas this value was only 77% for two PCs. We believe that adding a third PC is well worth the additional computational time for clustering.

A portion of the differences between the various types of retrievals is due to the differing number of FOVs that were averaged. For example, MAN retrievals were made for as few as 8 (but not more than 16) FOVs, while CLS retrievals were made from between 16 and 193 FOVs. This variation produces different amounts of noise reduction and probably is a factor in causing the MAN retrievals to appear somewhat "noisy."

Solid lines on the top two thermodynamic diagrams (Figs. 3a,b) denote cluster-derived retrievals at the driest and nearby moist sites (denoted *M*, see locations in Fig. 2d). One should note that the similarity between the manual and cluster profiles extends vertically through the entire soundings. Finally, Fig. 3c shows that the driest CLS retrieval with a PW of 9.8 mm has considerably colder dewpoints than the first guess from which it was derived (the PW is 21.7 mm). A similar contrast occurs between the driest MAN retrieval and its first guess (not shown).

b. 11 July 1989

No retrievals could be made during the remainder of 10 July because GOES VAS performed rapid interval scans. By the following morning, 11 July 1989, surface dewpoints over central Florida had increased 5°C to become approximately 25°C (not shown). At 850 hPa (Fig. 1b), radiosonde-derived dewpoints show that the air had become drier over extreme southeastern Florida but more humid over the central peninsula. Large-scale patterns of lower-tropospheric precipitable water (Fig. 1d) also show that central Florida now is relatively humid. This section examines retrievals from the cluster and manual approaches for 1018 UTC 11 July.

The analysis of 54 manually derived VAS dewpoints at 850 hPa for 1018 UTC 11 July is shown in Fig. 6a. The mesoscale dry feature from the day before (Fig. 2a) now is considerably weaker (only −3°C), and it appears to have moved westward due to the large-scale easterly flow over the area (Fig. 1). Most of southeastern Florida is drier than the day before, with dewpoints as cold as −4°C. Conversely, values just west of Cape Canaveral have increased nearly 20°C during the past 24 h. This dewpoint analysis is consistent with that of total column precipitable water from the split window algorithm (Fig. 4b). Both show relatively dry air near Tampa and over the southeastern portion of the peninsula.

Thirty-nine cluster-derived retrievals are plotted in Fig. 6b. They were prepared from 26 original clusters as described for the previous day. Compared to the manual approach, the analysis of cluster-derived dewpoints indicates slightly drier conditions over southeastern Florida. Although the CLS retrievals do not depict the closed mesoscale dry region just east of Tampa, that area is shown to be relatively dry. Both versions continue to indicate the relatively dry air over extreme southern Georgia and the more humid air over northern Florida.

Figure 7a shows retrievals near the driest manual site located just east of Tampa (see Fig. 6a). The manual (dashed) and cluster (solid) retrievals show good agreement at all levels. In addition they both indicate that the driest air now is located near 700 hPa and is not as deep as the day before (Fig. 3a). Figure 7b compares CLS retrievals on 10 and 11 July at point *X* (Figs. 2d and 6b) that is located just north of a Tampa–Cape Canaveral line. The dewpoint profile on 11 July (dashed) indicates more humid conditions than the day before (solid). South of this line, however, the CLS retrievals (Fig. 7c) at point *Y* (Figs. 2d and 6b) show that the air continues to be relatively dry.

We have compared MAN, BLK, and CLS retrievals for additional times and levels (not shown). Retrievals derived from the objective clustering procedure are similar to those obtained using the more time consuming and subjective manual method. On the other hand, BLK retrievals exhibit weaker horizontal gradients be-

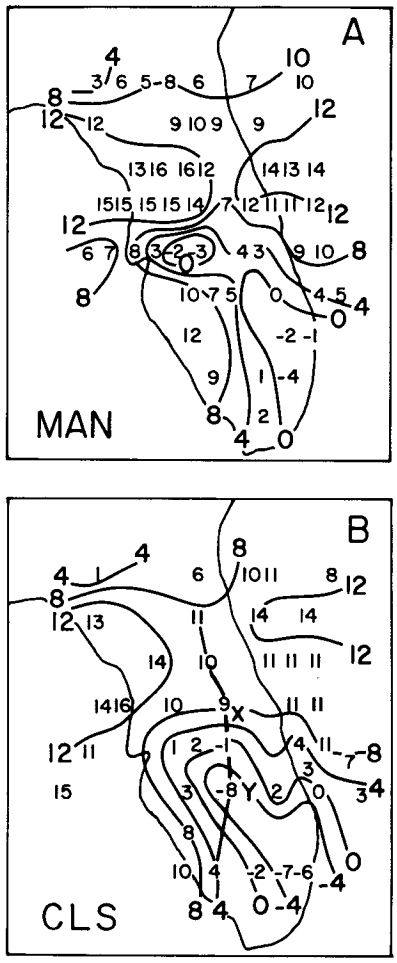

FIG. 6. As in Fig. 2 but for 1018 UTC 11 July 1989. (a) and (b) Manual and cluster-derived retrievals, respectively. Points *X* and *Y* are sounding locations shown in Fig. 7. The solid line segments in (b) represent the axis of a cross section shown in Fig. 8b.

cause FOVs are averaged without regard to meteorological features. Furthermore, the size (11 × 11) and shape of the blocks are fixed, except when cloud contaminated and data void ("Venetian blind") FOVs are deleted.

c. Preconvective environments

VAS retrievals can be used to investigate the potential for deep convection on 10–11 July. We calculated various parameters from the MAN and CLS retrievals for this purpose. Since results of the two versions were similar (as were the retrievals themselves), only the CLS-derived parameters are presented. Figure 8a is a cross section of CLS-derived equivalent potential temperature for 1018 UTC 10 July. Its axis runs north–south, passing through the driest point at 850 hPa (see axis in Fig. 2d). The values of potential temperature decrease with altitude due to the strong vertical gradient

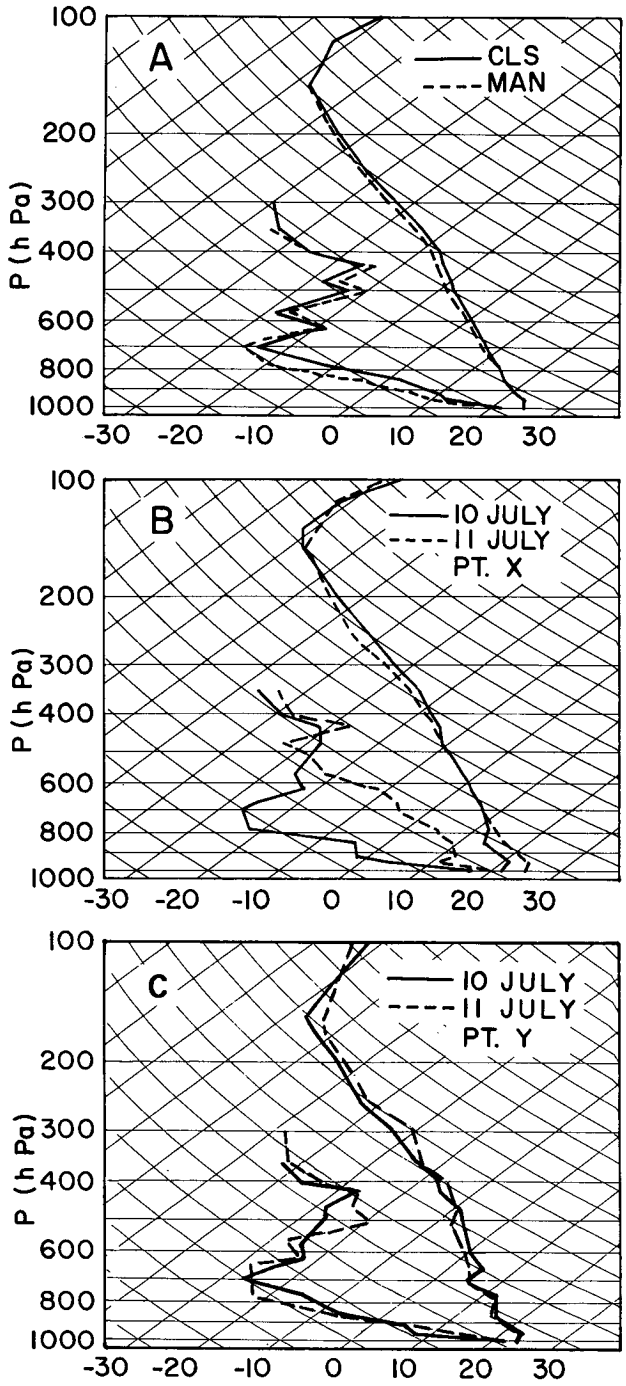

FIG. 7. Skew T–log$p$ diagrams of various retrievals. (a) The driest manual site in Fig. 6a and the closest corresponding cluster site in Fig. 6b. (b) The cluster-derived retrievals for point X at 1018 UTC 10 July in Fig. 2d (solid) and at 1018 UTC 11 July in Fig. 6b (dashed). (c) Similar to panel (b) but containing cluster-derived retrievals for point Y in Figs. 2d and 6b.

of humidity (Fig. 3a). Although this convective instability can be associated with intense thunderstorms over the Midwest, a dry middle troposphere inhibits thunderstorm development over Florida (e.g., Burpee 1979; Lopez et al. 1984; Fuelberg and Biggar 1994).

Figure 9 shows K indices (KIs, George 1960) calculated from the CLS retrievals. The KI includes the effects of temperature lapse rate as well as dewpoints at 850 and 700 hPa. The large negative values (reaching −33°C) suggest that central Florida will not experience thunderstorms during the afternoon of 10 July. The positive areas over northern Florida and extreme South Florida are more likely to support convection since they denote more humid conditions (Fig. 2d). Fuelberg and Biggar (1994) found that the surface-based lifted index was a valuable tool for assessing convective potential over North Florida. However, that index would not be as useful in the current case since humidity at 700 mb is not considered.

GOES visible imagery for the afternoon of 10 July (see example in Fig. 10a) shows that central Florida remains relatively cloud free during the entire afternoon. The clouds that are present generally are concentrated along the sea breeze front that is most evident along the eastern coast. Thunderstorms form only over extreme northern and southern Florida where the air is most humid. However, none of the convection is intense or widespread.

Conditions over central Florida are more conducive to thunderstorm development on 11 July (Figs. 6 and 7). The cross section of equivalent potential temper-

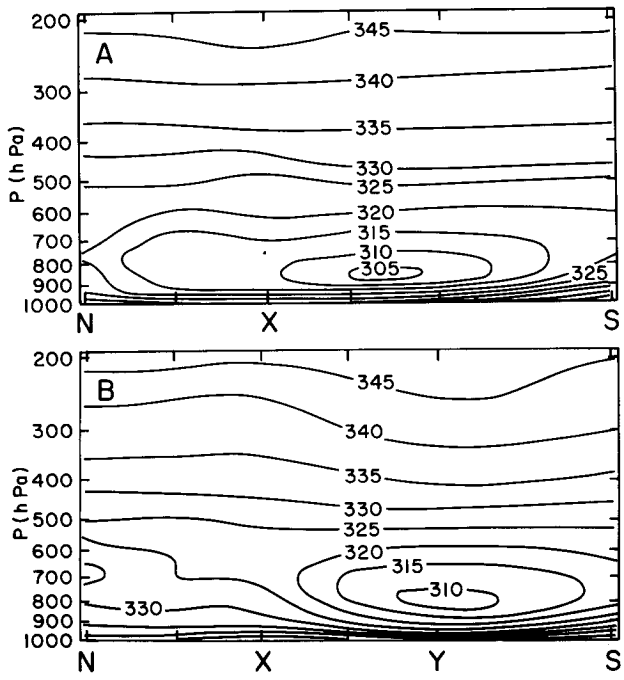

FIG. 8. Cross sections of equivalent potential temperature (K) from cluster retrievals. Both sections pass through the dry feature: (a) 1018 UTC 10 July (see axis in Fig. 2d); (b) 1018 UTC 11 July (see axis in Fig. 6b). Tick marks along the abscissa denote retrieval locations. Points X in Fig. 2d and X and Y in Fig. 6b are indicated.

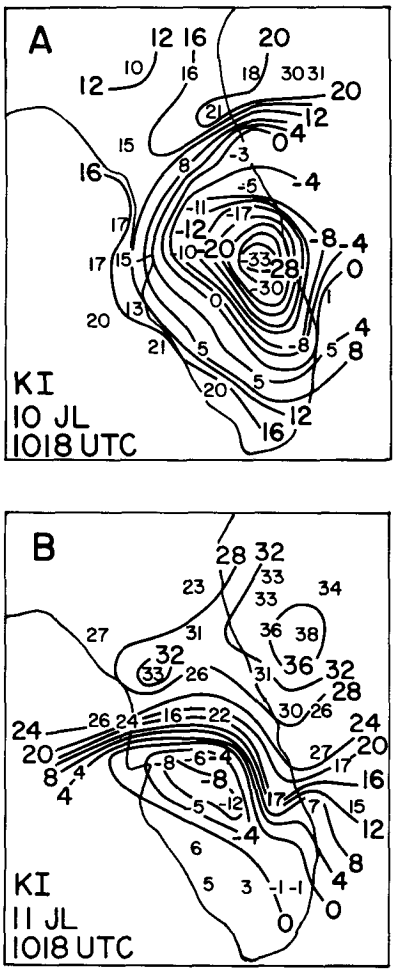

FIG. 9. Subjective analyses of the K index (°C) derived from cluster retrievals: (a) and (b) 1018 UTC 10 July and 11 July, respectively.

ature (Fig. 8b, along axis in Fig. 6b) continues to show values decreasing with altitude in the lower troposphere. However, the convective instability is not as intense as the day before, especially over the northern part of the region. This is consistent with the greater low- to middle-level humidity that was noted previously (Figs. 6b and 7b).

Cluster-derived KIs for 1018 UTC 11 July (Fig. 9b) also show considerable change from the previous day. The area just southeast of Tampa is least likely to support deep convection; however, the smallest value of −12°C is much greater than the −33°C of the day before. A representative sounding for the area (Fig. 7c, point Y in Fig. 6b) shows that the air continues to be relatively dry. A strong gradient of KI extends across central Florida, with positive values to the north. The greatest value of 33°C represents approximately a 70% probability of thunderstorm development (Sadowski and Rieck 1977). A sounding for this area (dashed in Fig. 7b, point X in Fig. 6b) shows that conditions are more humid than further south (Fig. 7c) and that the area has moistened considerably from the day before.

Cumulus clouds develop by mid morning on 11 June. By 1700 UTC (not shown), thunderstorms are occurring near Cape Canaveral and Tampa in association with sea-breeze fronts along both the east and west coasts. Areal coverage of the storms increases rapidly, and by 1900 UTC (Fig. 10b), much of central Florida is covered by intense convection. Storms never occur over north Florida; however, weaker thunderstorms develop in the Miami area around 2000 UTC, several hours after they had formed over the central peninsula. The region of storm coverage agrees closely with the locations of large KIs and the most humid lower troposphere (Figs. 6 and 9).

4. Conclusions

VAS physical retrievals made using a clustering procedure have been compared with those from a manual approach and a "blocking" procedure. The period of study, 10–11 July 1989, contained intense gradients of humidity over central Florida. Retrievals from each technique depicted a mesoscale area of very dry lower-tropospheric air over central Florida. The locations and strengths of the dry region were comparable for the manual and cluster approaches. However, the blocking procedure that is used operationally by NESDIS produced retrievals with weaker humidity gradients. The evolution of the dry region over central Florida was closely related to convective activity over the area.

VAS retrieval sites can be selected manually such that intense humidity gradients are detected. However, that subjective process is time consuming and therefore not appropriate for operational use. For the current case, the clustering procedure produced comparable results without human intervention.

The clustering approach can be utilized with improved IR data from *GOES-8* and beyond, and we believe that the procedure deserves careful consideration for future use in operational severe storms forecasting. The current clustering methodology is not suitable for operational use because of the stringent time constraints of those activities. However, a new, fast-clustering technique is being developed as a result of this research. This faster clustering still will use PCs to differentiate significant changes from noise, but it will not be constrained by the iterative technique used to put cluster members into the clusters. In addition, an objective analysis method (not used or discussed in this paper) has been developed along with the clustering technique. This objective analysis scheme considers the cluster designation of a given location as well as the designations of adjacent locations in PC space. Retrievals are produced for each cluster, with the results spread over the entire field by considering the distance from the cluster center and the distance to centers of adjacent clusters. In other words, the entire field is in-

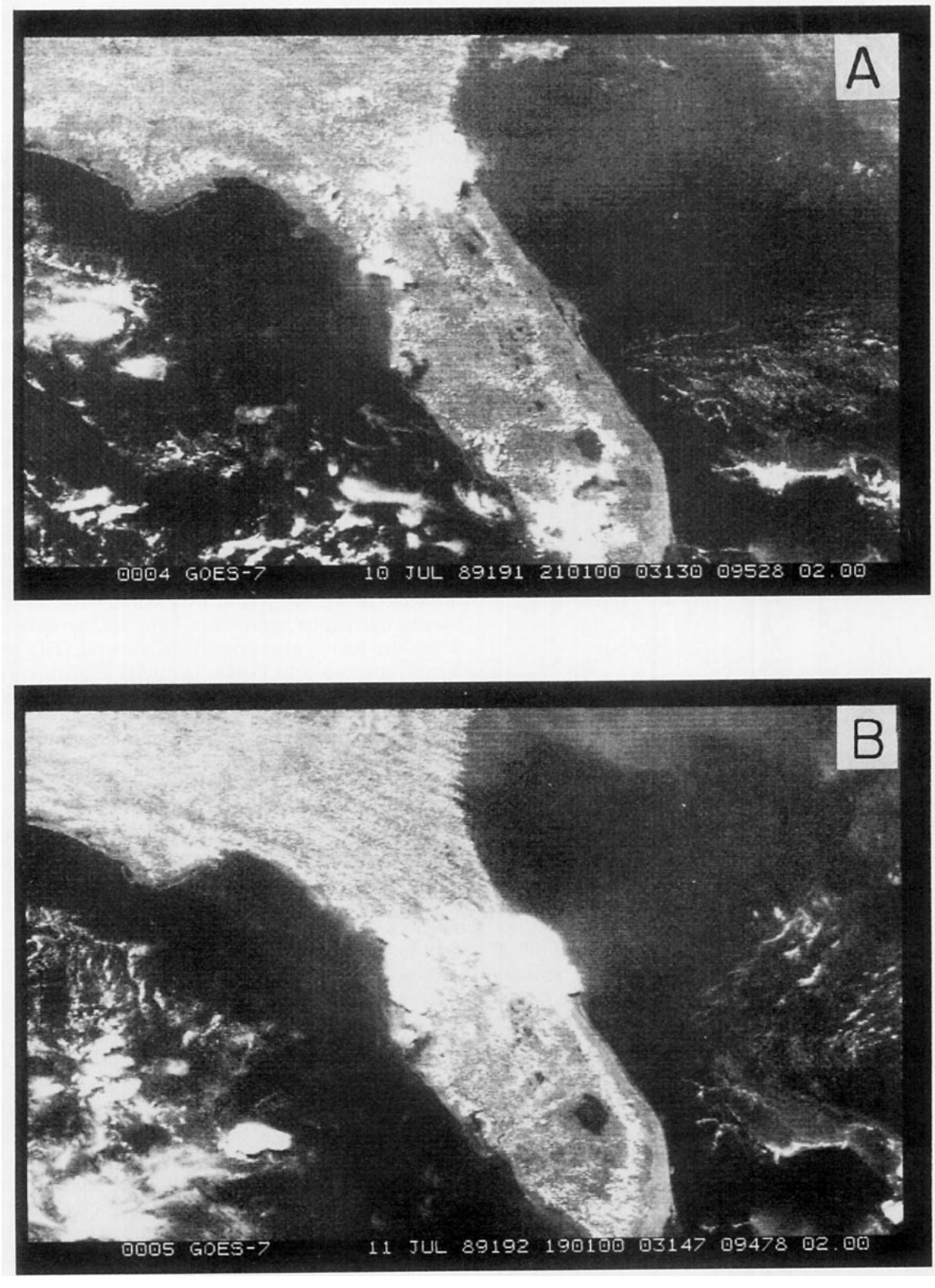

FIG. 10. GOES 1-km visible images for (a) 2101 UTC 10 July and (b) 1900 UTC 11 July 1989.

terpolated between clusters in a continuous fashion, so that each member of a cluster has mainly the characteristics of that cluster retrieval but also characteristics of retrievals from adjacent clusters. Only with these improvements will clustering be able to handle the volume of data and the speed needed to meet operational time constraints.

Acknowledgments. The research at FSU was supported by NASA Grant NAG10-0047 under the auspices of the Kennedy Space Center. Mr. James Nicholson, our technical monitor, was very helpful throughout the investigation. Additional support was provided by NASA Grant NAG8-942 through the Marshall Space Flight Center. The research at Colorado State was sponsored by NOAA Grant NA85RAH05045. We appreciate the assistance of Rick Knabb and Wayne Hoepner at FSU. The figures were drafted by Dewey Rudd (FSU). Dr. Christopher Hayden (NOAA/NESDIS) provided code for the VAS physical retrieval algorithm and answered many questions about its use.

REFERENCES

Baker, M. N., H. E. Fuelberg, and J. E. Ahlquist, 1993: Satellite-derived precipitable water over central Florida and its relation to thunderstorm development. Preprints, *17th Conf. on Severe Local Storms,* St. Louis, MO, Amer. Meteor. Soc., 88–92.

Burpee, R. W., 1979: Peninsula-scale convergence in the south Florida sea breeze. *Mon. Wea. Rev.*, **107,** 852–860.

Chesters, D., L. W. Uccellini, and W. D. Robinson, 1983: Low-level water vapor fields from the VISSR Atmospheric Sounder (VAS) "split window" channels. *J. Climate Appl. Meteor.*, **22,** 725–743.

——, W. D. Robinson, and L. W. Uccellini, 1987: Optimized retrievals of precipitable water from the VAS "split window." *J. Climate Appl. Meteor.*, **26,** 1059–1066.

Franklin, J. L., C. S. Velden, J. Kaplan, and C. M. Hayden, 1990: Some comparisons of VAS and dropwindsonde data over the subtropical Atlantic. *Mon. Wea. Rev.*, **118,** 1869–1887.

Fuelberg, H. E., and S. R. Olson, 1991: An assessment of VAS-derived retrievals and parameters used in thunderstorm forecasting. *Mon. Wea. Rev.*, **119,** 795–814.

——, and D. G. Biggar, 1994: The preconvective environment of summer thunderstorms over the Florida panhandle. *Wea. Forecasting,* **9,** 316–326.

Gauch, H. G., Jr., 1993: Prediction, parsimony, and noise. *Amer. Sci.*, **81,** 468–478.

George, J. J., 1960: *Weather Forecasting for Aeronautics.* Academic Press, 637 pp.

Hayden, C. M., 1988: GOES-VAS simultaneous temperature–moisture retrieval algorithm. *J. Appl. Meteor.*, **27,** 705–733.

Hillger, D. W., and T. H. Vonder Haar, 1988: Estimating noise levels of remotely sensed measurements from satellites using spatial structure analysis. *J. Atmos. Oceanic Technol.*, **5,** 206–214.

——, and J. F. W. Purdom, 1990: Clustering of satellite sounding radiances to enhance mesoscale meteorological retrievals. *J. Appl. Meteor.*, **29,** 1344–1351.

——, and J. F. Weaver, 1994: Analysis of mesoscale satellite soundings with and without clustering. Preprints, *Seventh Conf. on Satellite Meteorology and Oceanography,* Monterey, CA, Amer. Meteor. Soc., 501–504.

Hoepner, W. H., and H. E. Fuelberg, 1992: The use of VAS retrievals for thunderstorm forecasting at the Kennedy Space Center. Preprints, *Sixth Conf. on Satellite Meteorology and Oceanography,* Atlanta, GA, Amer. Meteor. Soc., J31–J35.

Jedlovec, G. J., 1985: An evaluation and comparison of vertical profile data from the VISSR Atmospheric Sounder (VAS). *J. Atmos. Oceanic Technol.*, **2,** 559–581.

Lee, T. H., D. Chesters, and A. Mostek, 1983: The impact of conventional surface data upon VAS regression retrievals in the lower troposphere. *J. Climate Appl. Meteor.*, **22,** 1853–1874.

Lopez, R. E., P. T. Gannon, Sr., D. O. Blanchard, and C. C. Balch, 1984: Synoptic and regional circulation parameters associated with the degree of convective shower activity in south Florida. *Mon. Wea. Rev.*, **112,** 686–703.

Sadowski, A. F., and R. E. Rieck, 1977: Technical Procedures Bulletin No. 207: Stability Indices. National Weather Service, Silver Spring, MD, 8 pp.

Suomi, V. E., R. Fox, S. S. Limaye, and W. L. Smith, 1983: McIDAS III: A modern interactive data access and analysis system. *J. Climate Appl. Meteor.*, **22,** 766–778.

Swain, P. H., S. D. Vardeman, and J. C. Tilton, 1981: Contextual classification of multispectral image data. *Pattern Recognition,* **13,** 429–441.

Velden, C. S., W. L. Smith, and M. Mayfield, 1984: Application of VAS and TOVS to tropical cyclones. *Bull. Amer. Meteor. Soc.*, **65,** 1059–1067.